

# Cluster Temperature Evolution: The Mass-Temperature Relation

G. Mark Voit<sup>1</sup>

Space Telescope Science Institute  
3700 San Martin Drive  
Baltimore, MD 21218

## ABSTRACT

Evolution of the cluster temperature function is extremely sensitive to the mean matter density of the universe. Current measurements based on cluster temperature surveys indicate that  $\Omega_M \approx 0.3$  with a  $1\sigma$  statistical error  $\sim 0.1$ , but the systematic errors in this method are of comparable size. Many more high- $z$  cluster temperatures will be arriving from *Chandra* and *XMM* in the near future. In preparation for future cluster temperature surveys, this paper analyses the cluster mass-temperature relation, with the intention of identifying and reducing the systematic errors it introduces into measurements of cosmological parameters. We show that the usual derivation of this relation from spherical top-hat collapse is physically inconsistent and propose a more realistic derivation based on a hierarchical merging model that more faithfully reflects the gradual ceasing of cluster evolution in a low- $\Omega_M$  universe. We also analyze the effects of current systematic uncertainties in the  $M_{\text{vir}}-T_X$  relation and show that they introduce a systematic uncertainty of  $\sim 0.1$  in the best-fitting  $\Omega_M$ . Future improvements in the accuracy of the  $M_{\text{vir}}-T_X$  relation will most likely come from comparisons of predicted cluster temperature functions with temperature functions derived directly from large-scale structure simulations.

*Subject headings:* galaxies: clusters: general — X-rays: galaxies

---

<sup>1</sup>voit@stsci.edu

## 1. Introduction

Surveys of distant clusters of galaxies are now realizing their promise as cosmological indicators (e.g., Henry 1997; Eke et al. 1998; Borgani et al. 1999a; Donahue & Voit 1999). Because clusters are the largest virialized objects in the universe, and the latest objects to form in hierarchical models of structure formation, their rate of evolution is quite sensitive to cosmological parameters. However, because cluster masses are difficult to measure directly, a surrogate for cluster mass is usually used when comparing cluster observations to structure-formation models. In the X-ray regime, the simplest cluster observables are X-ray luminosity ( $L_X$ ) and emissivity-weighted temperature ( $T_X$ ). Temperature is more directly related to a cluster’s mass, but luminosity can also be mapped to mass via an  $L_X - T_X$  relation. In either case, the crucial link between models and observations is the mass-temperature relation.

Recent analyses of high-redshift cluster temperature functions from the *Einstein* Extended Medium-Sensitivity Survey (EMSS) have shown that the matter density of the universe probably lies in the range  $0.2 < \Omega_M < 0.7$  (Henry 1997; Donahue et al. 1998; Bahcall & Fan 1998; Eke et al. 1998; Donahue & Voit 1999; but see Blanchard & Bartlett 1998; Viana & Liddle 1999). Even though these conclusions are based on rather few clusters, the systematic errors in these measurements of  $\Omega_M$  are comparable to the statistical errors (Donahue & Voit 1999). With the flood of cluster temperature measurements expected over the next few years from *Chandra* and *XMM*, we will have the opportunity to measure  $\Omega_M$  much more precisely. If we are to take full advantage of these measurements, we will need to reduce the systematic errors that currently exist in the modeling. Here we concentrate on the uncertainties in the mass-temperature relation itself.

This paper analyzes the role of the mass-temperature relation in characterizing cluster temperature evolution. Section 2 outlines the formalism used to describe the evolution of the cluster mass function. Section 3 investigates the physics underlying the mass-temperature relation, showing that the standard derivation of this relation from spherical top-hat collapse is flawed and suggesting a new context for understanding the physical effects that govern this relation. Section 4 discusses how to normalize the mass-temperature relation and evaluates how severely uncertainties in this normalization affect measurements of cosmological parameters. Section 5 summarizes the paper.

## 2. Mass-Function Evolution

Numerical simulations have shown that the Press-Schechter formalism (Press & Schechter 1974) and its various extensions (e.g., Lacey & Cole 1993) characterize gravitationally driven structure formation with surprising fidelity, particularly on cluster scales (e.g., Lacey & Cole 1994; Eke, Cole, & Frenk 1996; Bryan & Norman 1998; Borgani et al. 1999a). Because of its successes, this formalism is often used to relate observed cluster temperature and luminosity functions to cosmological models (e.g., Henry & Arnaud 1991; Eke et al. 1996; Borgani et al. 1999a). While some recent large-scale simulations have shown that the Press-Schechter formula might be somewhat less successful at predicting the number density of the most massive clusters (e.g., Governato et al. 1999), we will assume in this paper that it is an exact description of the cluster mass function, because here we are more concerned with analyzing systematic problems with the mass-temperature relation.

This section briefly outlines the formalism we will employ for expressing the cluster mass function. We derive expressions for mass-function evolution in both open and flat universes, and we assess the effects of a cosmological constant on cluster evolution. Many of these results have been derived elsewhere; we compile them here as background for subsequent sections.

### 2.1. Press-Schechter Formalism

The Press-Schechter formalism for structure formation and its extensions describe how virialized objects grow from a field of initial density perturbations. One defines  $\delta(\mathbf{x}, t; M)$  to be the local fractional overdensity of the universe smoothed on mass scale  $M$  and centered on comoving point  $\mathbf{x}$  at time  $t$ . While these fluctuation amplitudes are linear, they grow in proportion to the function  $D(t)$ , which depends on  $\Omega_M$  and  $\Omega_\Lambda$ , and their rms amplitude on scale  $M$  can be expressed as  $\sigma(M)D(t)/D(t_0)$ . Ultimately, some of these fluctuations grow non-linear, and they are assumed to virialize when their amplitudes, extrapolated from the linear regime according to  $D(t)$ , exceed some critical threshold for virialization  $\delta_c(t)$ , which also depends on  $\Omega_M$  and  $\Omega_\Lambda$ . One can then trace the merger history of a mass parcel beginning at location  $\mathbf{x}$  from time  $t_1$  to the present by keeping track of the largest  $M$  for which  $\delta(\mathbf{x}, t_1; M)D(t)/D(t_1) > \delta_c(t)$ .

Assuming that the perturbations are Gaussian, we can assess the number density of virialized objects with mass  $> M$  by evaluating the quantity  $\nu_c(M, t) \equiv [\delta_c(t)/\sigma(M)][D(t_0)/D(t)]$ , which is the critical virialization threshold in units of the characteristic fluctuation amplitude. The probability that a given mass parcel

is part of a virialized structure of mass  $> M$  is then equal to  $\text{erfc}[\nu_c(M, t)/\sqrt{2}]$ , where  $\text{erfc}(q)$  is the complementary error function. Thus, the overall mass density in virialized objects exceeding mass  $M$  is

$$\rho(> M) = \rho_0 \text{erfc}\left(\frac{\nu_c}{\sqrt{2}}\right) = \frac{2\rho_0}{\sqrt{\pi}} \int_{\nu_c/\sqrt{2}}^{\infty} e^{-x^2} dx, \quad (1)$$

where  $\rho_0$  is the mean mass density of the universe. Differentiating this expression with respect to  $M$  and dividing the result by  $M$  yields the familiar Press-Schechter formula for the comoving differential number density  $dn$  of virialized objects within mass interval  $dM$ :

$$\frac{dn}{dM}(M, t) = \left(\frac{2}{\pi}\right)^{1/2} \frac{\Omega_M \rho_{\text{cr},0}}{M^2} \left| \frac{d \ln \sigma}{d \ln M} \right| \nu_c(M, t) \exp[-\nu_c^2(M, t)/2], \quad (2)$$

where  $\rho_{\text{cr},0} = 3H_0^2/8\pi G$  represents the present-day critical mass density.

The evolution of  $dn/dM$  depends solely on  $\nu_c(M, t)$ . At present, we have  $\nu_c(M, t_0) = \delta_c(t_0)/\sigma(M)$ , and in principle, we can determine  $\sigma(M)$  by fitting equation (2) to the current distribution of cluster masses. The function  $\sigma(M)$  can be approximated by a power law with index  $\alpha = (n + 3)/6$  on cluster scales, so that  $\sigma(M) = \sigma_8(M/M_8)^{-\alpha}$  with  $M_8 = (H_0^2 \Omega_M / 2G)(8 h^{-1} \text{Mpc})^3 = 6.0 \times 10^{14} \Omega_M h^{-1} M_\odot$ . Holding  $\sigma(M)$  fixed, we can project the current cluster mass distribution backward in time as long as we know the functions  $\delta_c(t)$  and  $D(t)$ . More specific expressions for  $\sigma(M)$  describe how  $n$  changes with the mass scale in CDM-like models, but the analytical simplicity of the power-law form better serves the illustrative purposes of this paper.

## 2.2. Cluster Evolution and $\Omega_M$

Massive cluster evolution is very sensitive to  $\Omega_M$  because the number density of large clusters depends exponentially on  $\nu_c^2$  which is  $\gg 1$ . Slight differences in the rate at which  $\nu_c$  evolves therefore translate into large differences in cluster evolution (e.g., Oukbir & Blanchard 1992; Eke et al. 1996; Viana & Liddle 1996). To illustrate how dramatic these differences can be, we will briefly outline the case of cluster evolution in an open universe with no cosmological constant.

Following Lacey & Cole's (1993) treatment of perturbation growth when  $\Omega_M < 1$  and  $\Omega_\Lambda = 0$  (see also the Appendix), we have  $\nu_c(M, t) = \omega(t)/\sigma(M)$  with

$$\omega(t) \equiv \delta_c(t)D(t_0)/D(t) = \frac{3}{2}D(t_0)[1 + (t_\Omega/t)^{2/3}], \quad (3)$$

where  $t_\Omega = \pi\Omega_M/H_0(1 - \Omega_M)^{3/2}$ . Normalizing the present value of  $\nu_c$  at some fiducial mass scale  $M_0$ , we can write

$$\nu_c(M, t) = \nu_c(M_0, t_0) \left( \frac{M}{M_0} \right)^\alpha \frac{1 + (t_\Omega/t)^{2/3}}{1 + (t_\Omega/t_0)^{2/3}} . \quad (4)$$

Because the cluster number density at mass scale  $M_0$  obeys  $dn/dM \propto \nu_c \exp(-\nu_c^2/2)$ , we can use this equation to gauge how rapidly clusters at this mass scale evolve.

Figure 1 illustrates how sensitively the number-density evolution of massive clusters ( $M_0 \approx 5 \times 10^{14} h^{-1} M_\odot$ ) depends on  $\Omega_M$ . For the purposes of this illustration, we have adopted the  $\sigma_8$  fitting formulae of Eke et al. (1996) and have assumed that  $n = -1.5$  on this mass scale. In this example, the number density of clusters in a universe with  $\Omega_M = 0.8$  grows by about five orders of magnitude from  $z = 1$  to the present, a rapid rate of evolution that contrasts sharply with the single order of magnitude expected in a universe with  $\Omega_M = 0.2$ . Changing the perturbation spectrum within observationally allowed bounds changes the quantitative predictions somewhat, but the qualitative conclusion remains the same: the number density of massive clusters evolves much more rapidly for  $\Omega_M \sim 1$  than for  $\Omega_M \ll 1$ .

### 2.3. Cluster Evolution and $\Lambda$

Clusters evolve slightly more rapidly in a flat,  $\Omega_\Lambda > 0$  universe than they do in an open,  $\Omega_\Lambda = 0$  universe with the same value of  $\Omega_M$  (e.g., Eke et al. 1996). When a cosmological constant is operating, the universe's density remains close to critical later in time, promoting perturbation growth at lower redshifts. However, cluster evolution is considerably less sensitive to  $\Omega_\Lambda$  than it is to  $\Omega_M$ .

In order to characterize cluster evolution in a flat universe with  $\Omega_\Lambda > 0$  we require expressions for  $D(t)$  and  $\delta_c(t)$ , which are derived in the Appendix. From these expressions we can construct the threshold function

$$\omega(t) = -9\xi_c(t)D(t_0) , \quad (5)$$

where  $\xi_c(t)$ , defined in the the Appendix, is proportional to the specific energy of a perturbation that collapses at time  $t$ . Normalizing  $\nu_c$  as before at the mass scale  $M_0$ , we can write

$$\nu_c(M, t) = \nu_c(M_0, t_0) \left( \frac{M}{M_0} \right)^\alpha \frac{\xi_c(t)}{\xi_c(t_0)} . \quad (6)$$

Plugging this expression into equation (2) then yields the desired formulae for cluster evolution.

The dotted lines in Figure 1 show how the number density of clusters at mass scale  $M_0$  evolves when  $\Omega_\Lambda > 0$ , for the  $\sigma_8$  normalization of Eke et al. (1996) and  $n = -1.5$ . Note that the rate of cluster evolution is quite insensitive to  $\Omega_\Lambda$ . In this particular case, the best-fitting  $\sigma_8$  for a flat universe is slightly higher than that for an open universe, which almost compensates for the slightly more rapid rate of evolution owing to  $\Lambda$ . In general, the best-fitting  $\Omega_M$  in an open universe is  $\sim 0.1$  higher than in a flat universe (e.g., Donahue & Voit 1999).

### 3. Theoretical Mass-Temperature Relations

The Press-Schechter formalism conveniently describes the rate at which virialized objects of mass  $M$  accumulate in the universe. If we could observe cluster masses directly, then comparisons between Press-Schechter predictions and observed cluster evolution would be simple. Several types of observables, such as X-ray temperature, cluster velocity dispersion, and weak lensing, are related to cluster masses, but linking these quantities with the proper Press-Schechter  $M$  values requires careful attention.

This section focuses on the relation between cluster mass and cluster temperature, the crucial relationship for linking X-ray observations of clusters to models of structure formation. We first outline the observational evidence for a well-behaved mass-temperature relationship. Then we analyze the standard derivation of the mass-temperature relation, which is based on collapse of a spherical top-hat perturbation to an isothermal sphere. This derivation yields a relation similar to the observed relation, but it fails to conserve energy, indicating that it omits important physical effects. In an effort to understand this relation more deeply, we present a model for cluster formation, drawn from the merging-halo formalism of Lacey & Cole (1993), which accounts for the fact that massive clusters accrete matter quasi-continuously. Analyzing clusters in this context enables us to identify the physical effects that make up for the lack of energy conservation. The primary advantage of the continuous formation model is that it more naturally reproduces the late-time evolution of clusters, and the section concludes by comparing predictions of cluster temperature evolution drawn from the continuous formation model with those from the spherical top-hat model.

### 3.1. Observational Evidence

Simple scaling arguments suggest that the X-ray temperatures of clusters ( $T_X$ ) should be directly related to their masses. One way to define a cluster’s mass is to specify a characteristic radius  $r_\Delta$  within which the mean density is  $\Delta$  times the critical density  $\rho_{\text{cr}}$ , so that  $M_\Delta = 4\pi r_\Delta^3 \rho_{\text{cr}} \Delta / 3$ . If all cluster potentials share the same density distribution,  $\rho(r/r_\Delta)$ , and the X-ray gas is isothermal, then  $T_X \propto M_\Delta / r_\Delta \propto M_\Delta^{2/3}$ . Numerical simulations of cluster formation demonstrate that this scaling ought to be remarkably tight, with a scatter of only 15 – 20% (Evrard, Metzler, & Navarro 1996; Bryan & Norman 1998). These simulations also provide normalizations for the mass-temperature relation that can be compared with actual clusters.

A recent observational investigation of the cluster mass-temperature relation at  $z \lesssim 0.1$  by Horner, Mushotsky, & Scharf (1999) supports the results of the simulations. They show that cluster masses derived from velocity dispersions (Girardi et al. 1998) agree well with those inferred from ASCA temperatures (Fukazawa 1997), using the scaling law from Evrard et al. (1996) at  $\Delta = 200$ :

$$M_{200} = (1.4 \times 10^{15} h^{-1} M_\odot) \left( \frac{T_X}{10 \text{ keV}} \right)^{3/2}. \quad (7)$$

The scatter in the observed mass-temperature relation is  $\sim 30\%$ , but it decreases by a factor of 2 for the clusters with the highest numbers of measured galaxy redshifts, suggesting that the scatter intrinsic to the mass-temperature relation is probably quite small. However, some concerns remain: a handful of outliers deviate from the standard relation by up to 50% and the mass normalization one finds from hydrostatic modeling of a subset of these clusters is 40% smaller (Horner et al. 1999).

Similar comparisons at higher redshifts are more difficult, but the available data indicate that the mass-temperature relation remains well-behaved. Hjorth, Oukbir, & van Kampen (1998) have compared masses derived from gravitational lensing analyses for 8 clusters at  $0.17 \leq z \leq 0.54$  with the X-ray temperatures of these clusters. Their best-fit mass-temperature relation agrees with the Evrard et al. (1996) scaling law within the observational errors, and they conclude that this scaling law can be used to measure masses to within 27%. For clusters at even higher redshifts ( $0.53 \leq z \leq 0.83$ ), Donahue et al. (1999) show that the observed relation between X-ray temperatures and cluster velocity dispersions remains consistent with the low- $z$  relation.

### 3.2. Virial Mass and the Late-Formation Approximation

The seemingly good behavior of the cluster mass-temperature relation is fortunate for those who wish to study cluster evolution with X-ray telescopes, but care must be taken when relating these temperature-derived masses to the virial masses demanded by the Press-Schechter formalism. From the simulations and observations, we know that the mass within a specified density contrast is straightforwardly related to temperature. However, the density contrast  $\Delta_{\text{vir}}$  corresponding to the virial radius depends in general on  $\Omega_M$  and  $\Omega_\Lambda$ . Thus, in order to characterize cluster evolution properly, we need to know how  $\Delta_{\text{vir}}(t; \Omega_M, \Omega_\Lambda)$  changes with time.

The usual approach to defining a cluster’s virial mass is to approximate cluster formation with the evolution of a spherical top-hat perturbation (e.g., Peebles 1993). Such a perturbation formally collapses to the origin at a particular moment ( $t_c$ ) which is taken to be the moment of virialization. The virialization time thus equals twice the time required for the perturbation to reach its turnaround radius ( $r_{\text{ta}}$ ). A naive application of the virial theorem, assuming that the perturbation is cold at maximum expansion, dictates that the cluster’s final potential energy ought to be twice its potential energy at turnaround. Hence, the cluster’s virial radius is assumed to be half its turnaround radius ( $r_{\text{vir}} = r_{\text{ta}}/2$ ). According to this prescription,  $\Delta_{\text{vir}}$  is a well-defined function of cosmic time and the parameters  $\Omega_M$  and  $\Omega_\Lambda$  (Lacey & Cole 1993; Kitayama & Suto 1996; Oukbir & Blanchard 1997). In the case of  $\Omega_\Lambda = 0$ , this function can be concisely expressed as  $\Delta_{\text{vir}} = 8\pi^2/(Ht)^2$ , where  $H$  is the Hubble constant at time  $t$ . If we additionally assume that each cluster we see at a given redshift  $z$  has just reached the moment of virialization, an assumption known as the late-formation approximation, then  $M_{\text{vir}} \propto T_X^{3/2} \rho_{\text{cr}}^{-1/2} \Delta_{\text{vir}}^{-1/2}$ .

In a critical  $\Omega_M = 1$  universe, the late-formation approximation is valid because massive clusters develop rapidly at all redshifts; the effective moment of virialization is always close to the moment of observation. However, in a universe with  $\Omega_M < 1$ , cluster formation is currently shutting down, and one must account for differences between the moment of virialization and the moment of observation. This problem grows most severe at late times in a  $\Omega_M \ll 1$  universe, because the quantity  $\rho_{\text{cr}} \Delta_{\text{vir}}$  as determined via the late-formation approximation declines indefinitely. The  $M_{\text{vir}}$  associated with a given  $T_X$  therefore rises steadily, even though cluster evolution has essentially stopped. This spurious late-time evolution of the  $M_{\text{vir}}-T_X$  relation is an undesirable artifact of the late-formation approximation.

One approach to solving this problem is to account explicitly for the difference between the moment of virialization and the moment of observation in the context of a merging-halo formalism for cluster growth (Viana & Liddle 1996; Kitayama & Suto 1996). Another



equivalent but mathematically simpler approach, which § 3.3 describes in detail, is to consider how the  $M_{\text{vir}}-T_X$  relation should evolve in a population of clusters that gradually accrete their matter over an extended period of time, a more realistic scenario for the growth of very massive clusters (Voit & Donahue 1998).

Calculating the normalization of the  $M_{\text{vir}}-T_X$  relation under the late-formation approximation is also somewhat problematic. Because a virialized cluster’s potential is approximately isothermal, one would like to approximate it with a singular isothermal sphere, truncated at radius  $r_{\text{vir}}$ , within which the mean density is  $\rho_{\text{cr}}\Delta_{\text{vir}}$ . The one-dimensional velocity dispersion within such a potential is  $\sigma_{\text{1D}}^2 = GM/2r_{\text{vir}}$  (Binney & Tremaine 1987), which leads to the following relation between virial mass and temperature:

$$\begin{aligned} kT_X &= \frac{GM^{2/3}\mu m_p}{2\beta} \left[ \frac{4\pi}{3} \rho_{\text{cr}} \Delta_{\text{vir}} \right]^{1/3} \\ &= (1.38 \text{ keV}) \beta^{-1} h^{2/3} M_{15}^{2/3} \Delta_{\text{vir}}^{1/3} \left[ \frac{\Omega_M}{\Omega_M(z)} \right]^{1/3} (1+z) \end{aligned} \quad (8)$$

where  $\beta = \mu m_p \sigma_{\text{1D}}^2 / kT_X$  and  $\mu m_p = 1 \times 10^{-24} \text{ g}$  is the mean mass per gas particle.

Comparisons of the  $M_{\text{vir}}-T_X$  relation in equation (8) with the masses and temperatures of simulated clusters indicate that  $\beta^{-1} \approx 0.8 - 1$  (e.g., Bryan & Norman 1998). This nearness of  $\beta$  to unity appears to validate the assumptions governing the derivation of equation (8), but the approximate agreement between this equation and the simulations turns out to be something of a coincidence. The total energy of a collapsing spherical top-hat perturbation is  $-3GM^2/5r_{\text{ta}}$ . After the collapsed perturbation virializes into an isothermal sphere, a naive application of the virial theorem that disregards boundary effects would place the total kinetic energy of the system at  $3GM^2/5r_{\text{ta}}$ , corresponding to  $\sigma_{\text{1D}}^2 = 2GM/5r_{\text{ta}}$ . The virial radius of the relaxed system would then be  $5r_{\text{ta}}/4$ , a factor of 2.5 larger than assumed in the derivation of equation (8), and its temperature would correspondingly be 2.5 times lower.

In fact, truncation of a virialized system at some  $r_{\text{vir}}$  implies the existence of a confining pressure, unaccounted for in the top-hat collapse model, that alters the usual virial relationship between potential and kinetic energy (e.g., Carlberg, Yee, & Ellingson 1997). In the case of a singular isothermal sphere, the total kinetic energy is three times the absolute value of the total energy. Thus, energy-conserving collapse of a spherical top-hat perturbation into a pressure-truncated singular isothermal sphere should yield  $\sigma_{\text{1D}}^2 = 6GM/5r_{\text{ta}}$ , implying  $r_{\text{vir}} = 5r_{\text{ta}}/12$  (e.g., Shapiro, Iliev, & Raga 1999). This result is close to the naive assumption that  $r_{\text{vir}} = r_{\text{ta}}/2$ , but it is valid only if a confining pressure is applied at the virial radius.

### 3.3. Continuously Forming Clusters

The inconsistencies in the top-hat, late-formation derivation of the  $M_{\text{vir}}-T_X$  relation outlined above indicate, perhaps unsurprisingly, that the top-hat collapse model excludes important physical effects that contribute to the normalization of the relation. In particular, the top-hat model accounts for neither the energy and mass accumulation during the early stages of cluster formation nor the confining effects of matter that continues to fall in, both of which significantly increase the temperature associated with a given mass. This section shows how these missing effects can be addressed in the context of a simple model in which massive clusters are allowed to form gradually, rather than instantaneously.

In hierarchical models for structure formation, the growth of the largest clusters is quasi-continuous. The most massive clusters are so rare that they almost never merge with another cluster of similar size (e.g., Lacey & Cole 1993). Rather, they grow by continually accumulating much smaller virialized objects. In the notation of § 2, their masses grow like  $M \propto \omega^{-3/(n+3)}$  (Lacey & Cole 1993; Voit & Donahue 1998). Because each bit of infalling matter carries with it a specific energy  $\epsilon$ , we can compute the virial energy  $-E$  of the cluster by integrating  $E = -\int \epsilon dM$ . The cluster temperature itself is proportional to  $E/M$ , so this integral also leads to a relation between virial mass and temperature.

Voit & Donahue (1998) treat the case of continuous cluster growth when  $\Omega_M < 1$  and  $\Omega_\Lambda = 0$ , finding that  $M \propto x^{-3m/5}$ , where  $x = 1 + (t_\Omega/t)^{2/3}$  and  $m = 5/(n+3)$ . Here we extend that calculation to include the constant of proportionality between energy and mass. Drawing on the Appendix, we express the specific energy of infalling matter at time  $t$  as

$$\epsilon(t) = -\frac{1}{2} \left( \frac{2\pi G M}{t_\Omega} \right)^{2/3} (x - 1) . \quad (9)$$

Thus, we obtain

$$\frac{E}{M} = \frac{3}{10} \frac{m}{m-1} \left( \frac{2\pi G}{t_\Omega} \right)^{2/3} M^{2/3} \left[ \left( \frac{t_\Omega}{t} \right)^{2/3} + \frac{1}{m} \right] . \quad (10)$$

In the limit of large  $m$ , which corresponds to the late-formation approximation, this expression reduces to

$$\frac{E}{M} = -\frac{3}{5} \epsilon(t) , \quad (11)$$

which is identical to the  $E/M$  ratio for a spherical top-hat perturbation of mass  $M$  that virializes at time  $t$ . A similar procedure yields the mass-temperature relation in a flat  $\Omega_\Lambda > 0$  universe. From the Appendix, we have  $\epsilon(t) \propto M^{2/3} \xi_c(t)$  and  $\omega(t) \propto -\xi_c(t)$ , giving

$$\frac{E}{M} = -\frac{3}{5} \frac{m}{m-1} \epsilon(t) , \quad (12)$$

which again reduces to  $-3\epsilon(t)/5$  in the limit of large  $m$ .

Two factors in equation (10) drive  $E/M$  higher than the late-formation value. The  $m/(m-1)$  factor, also present in equation (12), accounts for the effects of early infall; continuous cluster formation tends to create hotter clusters than top-hat formation because more of the mass is assembled early, at a higher mean density. For values of  $n$  typical of cluster scales ( $-2 \gtrsim n \gtrsim -1$ ), this factor ranges from 1.2 to 1.7. The  $1/m$  term in the bracketed factor of equation (10) accounts for the cessation of cluster formation when  $t \gg t_\Omega$ . At late times in an open universe,  $E/M$  should remain constant, but in the late-formation approximation  $E/M$  falls indefinitely because the fiducial density scale never stops dropping.

Relating  $E/M$  to temperature requires an expression for the relationship between the total virial energy  $-E$  and the total kinetic energy  $E_K$ . When an external pressure  $P$  confines the boundary of a spherically symmetric virialized system, the appropriate form of the virial theorem can be written

$$E_K = E + 4\pi P r_{\text{vir}}^3 . \quad (13)$$

If we take the velocity dispersion to be isothermal ( $\sigma_{\text{1D}} = \text{const.}$ ), then  $P = \rho(r_{\text{vir}})\sigma_{\text{1D}}^2$ , and

$$E_K = \frac{\bar{\rho}}{\bar{\rho} - 2\rho(r_{\text{vir}})} E , \quad (14)$$

where  $\bar{\rho}$  is the mean density within the virial radius. In this formulation, the ratio  $E_K/E$  depends on the shape of the potential within  $r_{\text{vir}}$ . If the local density is negligible at  $r_{\text{vir}}$ , then the confining pressure is effectively zero and  $E_K = E$ . If the potential strictly obeys  $\rho \propto r^{-2}$ , then  $E_K = 3E$ .

Because we wish to derive an approximate mass-temperature relation for comparison with observations and simulations giving the temperature and mass of a cluster within  $r_{200}$ , let us compute  $E_K/E$  for the “universal” density profile of Navarro, Frenk, & White (1997), truncated at  $r_{200}$ , under the assumption that  $\sigma_{\text{1D}}$  is constant. The ratio of mean density to local density within  $r_{200}$  is then

$$\frac{\bar{\rho}}{\rho(r_{200})} = 3 \frac{(1+c)^2}{c^2} \ln \left[ (1+c) - \frac{c}{1+c} \right] , \quad (15)$$

where  $c$  is a parameter that quantifies the concentration of matter toward the cluster’s center. Simulations by Eke, Navarro, & Frenk (1998) show that  $c \approx 4 - 6.5$  for clusters at  $0 < z < 1$  in a  $\Omega_{\text{M}} = 0.3$ ,  $\Omega_{\Lambda} = 0.7$  universe, and simulations of cluster formation by Navarro et al. (1997) show that the most massive clusters in critical universes exhibit

similar levels of concentration. Values of  $c \sim 5$  lead to density contrast factors  $\approx 4$  and  $E_K/E \approx 2$ .

An intriguing alternative approach by Shapiro et al. (1999) investigates the post-collapse structures of clusters by seeking the minimum-energy solution among a family of non-singular truncated isothermal spheres. The minimum-energy solution turns out to closely resemble the self-similar spherical infall solution of Bertschinger (1985). Because the truncation radius of this minimum-energy isothermal sphere is nearly equal to the accretion-shock radius of the infall solution, Shapiro et al. (1999) suggest that continual infall naturally maintains the confining pressure on the virialized isothermal sphere. In this model, the density contrast factor at the truncation radius is 3.73, and  $E_K/E = 2.17$ .

Taken together, the effects of early accretion and pressure confinement make up for the lack of energy conservation in the top-hat, late-formation derivation of equation (8). In the early-time limit ( $t \ll t_\Omega$ ), equation (10) yields the following mass-temperature relation:

$$kT_X = \left[ \frac{2}{5} \frac{m}{m-1} \frac{E_K}{E} \right] \frac{GM^{2/3} \mu m_p}{2\beta} \left( \frac{4\pi}{3} \rho_{\text{cr}} \Delta_{\text{vir}} \right)^{1/3}. \quad (16)$$

When  $n \approx -2$  and  $E_K/E \approx 2$ , the prefactor in brackets is close to unity, making this expression nearly identical to equation (8).

The lesson here is that the assumptions underlying equation (8) are physically unsound. The approximate agreement between the  $M_{\text{vir}}-T_X$  normalization derived via the top-hat collapse model and those derived from simulations and observations is largely coincidental. As long as  $\Omega_M$  is not very small, the time-dependent factors in equations (8) and (10) do not differ by a large factor. However, because equation (10) more faithfully reflects the behavior of cluster formation in all the appropriate limits, we prefer to base the  $M_{\text{vir}}-T_X$  relation on the continuous-formation model.

### 3.4. Late-Formation vs. Continuous-Formation

The  $M_{\text{vir}}-T_X$  relations in equation (8), derived using the late-formation approximation, and equation (10), derived using the continuous-formation approximation, differ in both normalization and time-dependent behavior. The following section will discuss the importance of properly normalizing the  $M_{\text{vir}}-T_X$  relation. Here we wish to examine how differences in time-dependence alone translate into different predictions for cluster evolution. In order to isolate the time-dependent behavior, we can identically normalize both  $M_{\text{vir}}-T_X$  relations to equation (7) at  $z = 0$  and compare the resulting cluster temperature functions.

Figure 2 shows the evolution of the temperature function for 8 keV clusters, given the  $\sigma_8$  normalization of Eke et al. (1996). Because the  $M_{\text{vir}}-T_X$  relation evolves less strongly in the continuous-formation case, the rise in cluster temperature at a given mass as  $z$  increases does not compensate as fully for the drop in the number of clusters at that mass. The evolution of the temperature function at a given value of  $\Omega_M$  is therefore stronger in the continuous-formation case (see also Viana & Liddle 1999). Correspondingly, the best-fitting  $\Omega_M$  to a given observed amount of cluster evolution will be lower. In this particular case, the difference amounts to  $\sim 0.1$  in  $\Omega_M$  for a best-fitting  $\Omega_M \approx 0.3$ .

Because the statistical errors in  $\Omega_M$  derived from cluster temperature evolution are also  $\sim 0.1$ , this discrepancy between the late-formation and continuous-formation approximations will need to be resolved if we are to take full advantage of the cluster temperature measurements expected from *Chandra* and *XMM*. The best way to proceed will be to test how well these temperature-function predictions represent the results of large-scale structure simulations. However, cluster temperature functions will have to be extracted directly from the simulated data, without resorting to a mass-temperature conversion step, presumably by using the cluster-particle velocity dispersion as a surrogate for cluster temperature.

#### 4. Normalization of the $M_{\text{vir}}-T_X$ Relation

Both the top-hat and continuous-formation derivations of the  $M_{\text{vir}}-T_X$  relation given in the previous section have holes which must be plugged with knowledge gained from simulations. In fact, any such spherically symmetric representation glosses over aspects of cluster formation that are inherently three-dimensional. Thus, it seems wise to normalize these analytical expressions to the results of numerical simulations. This procedure appears simple enough, but one must bear in mind that the normalization depends on  $\Omega_M$  and that simulations have been done only for a few particular values of  $\Omega_M$ . Here we explain how we choose to normalize the  $M_{\text{vir}}-T_X$  relation then investigate the consequences of an offset in the normalization.

##### 4.1. Normalizing to Simulations

Because of the good agreement between the observational compilation of Horner et al. (1999) and the simulations of Evrard et al. (1996), we would like to normalize the  $M_{\text{vir}}-T_X$  relation accordingly. Applying the time-dependence factors derived for continuously forming

clusters to the empirical mass-temperature relation in equation (7) thus gives

$$kT_X = (8.0 \text{ keV}) \left( \frac{M}{10^{15} h^{-1} M_\odot} \right)^{2/3} \left[ \frac{(t_\Omega/t)^{2/3} + 1/m}{(t_\Omega/t_0)^{2/3} + 1/m} \right] \quad (17)$$

and

$$kT_X = (8.0 \text{ keV}) \left( \frac{M}{10^{15} h^{-1} M_\odot} \right)^{2/3} \frac{\xi_c(t)}{\xi_c(t_0)} \quad (18)$$

for open and flat universes, respectively.

Figure 3 compares this empirical normalization with the normalizations of the  $M_{\text{vir}}-T_X$  relations derived by Eke et al. (1996) and Voit & Donahue (1998) at  $z = 0$ , assuming  $\Omega_\Lambda = 0$ . The dashed line indicates the normalization given in equation (7), which is presumed to be independent of  $\Omega_M$ . The curve labeled “late formation” shows the normalization of equation (8), derived from the top-hat, late-formation model. This normalization drops steadily with decreasing  $\Omega_M$  because the density contrast factor  $\Delta_{\text{vir}}$  grows smaller as  $\Omega_M$  declines. Clusters modelled in this way are therefore less compact and cooler than one would expect from the critical density alone. When  $\Omega_M = 1$ , this normalization is only 4% below the empirical value, but if  $\Omega_M = 0.2$ , it lies 20% below this value, corresponding to mass discrepancies of 6% and 30%, respectively.

The behavior of the normalizations derived from continuous-formation models is more complicated. Voit & Donahue (1998) normalized these relations to the Eke et al. (1996) relation at  $\Omega_M = 1$  to simplify comparisons. For  $\Omega_M \lesssim 1$ , they are lower than at  $\Omega_M = 1$  for the same reason as in the late-formation model. However, if  $\Omega_M \ll 1$ , cluster formation happened long before  $z \approx 0$ , when the universe was considerably denser. Clusters are therefore denser and hotter than one would expect from the current critical density. As a result, the temperature normalization of the  $n = -2$  case deviates by less than 10% over the range  $0.2 < \Omega_M < 1.0$ . In the  $n = -1$  case the normalization is actually 18% higher than the empirical value (27% in mass) at  $\Omega_M = 0.2$ .

This comparison illustrates why the procedure of normalizing the  $M_{\text{vir}}-T_X$  relation to simulations is imperfect. In general, we expect this normalization to vary with  $\Omega_M$  in a way that depends on  $n$ . Given that we have simulations for only a handful of cosmological models, how do we unambiguously normalize these relations? Furthermore, different choices for extrapolating this normalization to other values of  $\Omega_M$  can lead to normalizations that differ by as much as 40% in temperature (60% in mass) at a given value of  $\Omega_M$ . Because of these uncertainties in the normalization of the  $M_{\text{vir}}-T_X$  relation, it is important to understand how offsets in the normalization affect cosmological parameters derived from the cluster temperature function.

## 4.2. Normalization Offset and $\sigma_8$

The  $M_{\text{vir}}-T_X$  relation is invoked twice in the usual derivation of  $\sigma_8$  from the low-redshift temperature function. In both instances, an overestimate of the mass associated with a given temperature drives the best-fitting value of  $\sigma_8$  higher. For example, a 50% offset in the mass normalization changes  $\sigma_8$  by about 15%. Systematic uncertainties in the  $M_{\text{vir}}-T_X$  relation therefore lead to systematic uncertainties in  $\sigma_8$ , limiting the usefulness of the temperature function as a tool to measure the perturbation amplitude.

The first place the  $M_{\text{vir}}-T_X$  relation enters is in the conversion of the theoretical cluster mass function  $dn/dM$  in equation (2) to the cluster temperature function

$$\frac{dn}{dT}(T, t) = \frac{3}{2} \left( \frac{2}{\pi} \right)^{1/2} \frac{\Omega_M \rho_{\text{cr},0}}{T M(T, t)} \left| \frac{d \ln \sigma}{d \ln M} \right| \nu_c[M(T, t), t] \exp\{-\nu_c^2[M(T, t), t]/2\} . \quad (19)$$

An  $M_{\text{vir}}-T_X$  relation that overestimates  $M(T)$  by a fractional amount  $\delta_M$  will underpredict the density  $dn/dT$  by the same fractional amount. This source of error drives the best-fitting value of  $\nu_c$  lower by a fractional amount  $\delta_\nu \approx -\delta_M/(\nu_c^2 - 1)$ .

Once  $\nu_c(T)$  has been derived over a given range of temperatures, one can determine  $\sigma(T) = \delta_c(t_0)/\nu_c(T)$ . These  $\sigma$  values will be too high by a fraction  $\approx \delta_M/(\nu_c^2 - 1)$  if there is a normalization offset. Conversion of  $\sigma(T)$  to  $\sigma(M)$  contributes another term to the systematic error budget. If  $M(T)$  is overestimated, the mismapping of temperature to mass inflates  $\sigma_8$  by a fractional amount  $\approx \alpha \delta_M$ .

As an example of these effects, consider the derivation of  $\sigma_8$  from the abundance of  $> 5$  keV clusters. Markevitch (1998) finds that the number density of such clusters at  $z \sim 0$  is  $\approx 7.0 \times 10^{-7} h^3 \text{Mpc}^{-3}$ . According to the mass-temperature relation in equation (7), the mass of a 5 keV cluster is  $5.0 \times 10^{14} h^{-1} M_\odot$ , leading to an overall mass density  $\rho(> 5 \text{ keV}) \approx 2.3 \times 10^{-32} h^2 \text{g cm}^{-3}$  in such objects. Plugging this value into equation (1) and solving for  $\nu_c$  yields  $\nu_c(5 \text{ keV}) \approx 3.2$  for  $\Omega_M = 1$  and  $\nu_c(5 \text{ keV}) \approx 2.8$  for  $\Omega_M = 0.3$ , numbers that are consistent with more rigorous fits to cluster temperature data using a similar mass-temperature relation (Donahue & Voit 1999).

Conversion of these  $\nu_c$  values to  $\sigma_8$  values depends on the shape of the initial perturbation spectrum and the value of the virialization threshold  $\delta_c$ . For the purposes of this analysis, we will assume that  $\delta_c$  is known perfectly, implying that  $\sigma(5.0 \times 10^{14} h^{-1} M_\odot) \approx 0.53$  for  $\Omega_M = 1.0$  and  $\sigma(5.0 \times 10^{14} h^{-1} M_\odot) \approx 0.59$  for  $\Omega_M = 0.3$ . Extrapolating along the mass spectrum assuming, for example, that  $n = -1.5$  then leads to  $\sigma_8 \approx 0.51$  for  $\Omega_M = 1.0$  and  $\sigma_8 \approx 0.76$  for  $\Omega_M = 0.3$ .

Now let us inflate the normalization of the mass-temperature relation by 50% in mass.

The overall mass density in objects  $> 5$  keV rises to  $\rho(> 5 \text{ keV}) \approx 3.5 \times 10^{-32} h^2 \text{ g cm}^{-3}$ , yielding  $\nu_c(5 \text{ keV}) \approx 3.1$  for  $\Omega_M = 1$  and  $\nu_c(5 \text{ keV}) \approx 2.7$  for  $\Omega_M = 0.3$ . Because 5 keV corresponds to  $7.5 \times 10^{14} h^{-1} M_\odot$  under the alternative normalization, we now have  $\sigma(7.5 \times 10^{14} h^{-1} M_\odot) \approx 0.54$  for  $\Omega_M = 1.0$  and  $\sigma(7.5 \times 10^{14} h^{-1} M_\odot) \approx 0.61$  for  $\Omega_M = 0.3$ . Extrapolation to  $\sigma_8$ , again assuming  $n = -1.5$ , gives  $\sigma_8 \approx 0.58$  for  $\Omega_M = 1.0$  and  $\sigma_8 \approx 0.87$  for  $\Omega_M = 0.3$ . Note that these systematic changes, of order 15%, exceed the typically quoted measurement errors for  $\sigma_8$  at a fixed value of  $\Omega_M$ .

Additional uncertainty in the derived value of  $\sigma_8$  can arise from uncertainty in the slope  $n$  of the perturbation spectrum. For example, the  $n \approx -2.3$  slope derived from the Markevitch cluster sample (Markevitch 1998; Donahue & Voit 1999) leads to a considerably lower derived value of  $\sigma_8$  when  $\Omega_M \ll 1$ . In the case of  $\Omega_M = 0.3$ , a measurement of  $\sigma(5.0 \times 10^{14} h^{-1} M_\odot) \approx 0.59$  extrapolates to  $\sigma_8 \approx 0.66$ , corresponding to clusters of temperature  $\sim 2.5$  keV, below the temperature limit of the sample. Blanchard et al. (1999) have recently argued that the Markevitch sample is incomplete at low temperatures, implying  $n > -2.3$ . That is probably why the best-fitting  $\sigma_8$  values of Donahue & Voit (1999), based primarily on the Markevitch clusters, seem unusually low. (Errors on  $\sigma_8$  quoted in that paper refer only to the statistical errors in  $\sigma_8$  at the best-fitting value of  $\Omega_M$ .) Ideally, one would like to measure  $\sigma_8$  from the number density of clusters at temperatures corresponding to the appropriate mass scale, but to do this, one first needs a reliable  $M_{\text{vir}}-T_X$  relation, in addition to a well constrained value of  $\Omega_M$ .

The upshot of this analysis is that  $\sigma_8$  values derived from the cluster temperature function contain systematic errors that depend on the mass-temperature relation. These systematic errors are currently comparable to the measurement errors. Until the  $M_{\text{vir}}-T_X$  relation is better understood,  $\sigma_8$  values derived from the cluster temperature function will have to be treated with caution. Conversely, predictions of cluster temperature functions that invoke  $\sigma_8$  values derived from other kinds of data will also contain systematic errors owing to normalization uncertainties in the  $M_{\text{vir}}-T_X$  relation.

### 4.3. Normalization Offset and $\Omega_M$

The systematic problems discussed above in relating  $\sigma_8$  to  $dn/dT$  need not lead to unwarranted pessimism about deriving  $\Omega_M$  from the evolution of  $dn/dT$ . The key quantity in establishing the rate of cluster temperature evolution is not  $\sigma_8$ , but rather  $\nu_c(T, t_0)$ , whose systematic errors are considerably smaller,  $\sim 5\%$  instead of  $\sim 15\%$ . In order to evaluate the impact of a  $M_{\text{vir}}-T_X$  normalization offset on predictions of temperature evolution, we will first analyze the case of  $\Omega_M = 1$ , then consider how a normalization offset affects



measurements of  $\Omega_M$ .

When  $\Omega_M = 1$ , the time-dependent parts of  $M(T, t)$  and  $\nu(T, t)$  simplify to  $M \propto (1 + z)^{-3/2}$  and  $\nu_c \propto (1 + z)^{(2-3\alpha)/2}$ . The amount of cluster evolution at a fixed temperature  $T$  can therefore be written as

$$C(T, z) = \frac{\frac{dn}{dT}(T, z)}{\frac{dn}{dT}(T, 0)} = (1 + z)^{(5-3\alpha)/2} \exp\left\{-\frac{\nu_c^2(T, 0)}{2}[(1 + z)^{(2-3\alpha)} - 1]\right\} . \quad (20)$$

A fractional overestimate  $\delta_M$  of cluster masses thus leads to an underestimate of the amount of evolution by a factor  $\sim \exp\{\delta_M[(1 + z)^{2-3\alpha} - 1]\}$ . If the overestimate of cluster masses is 50%, this factor amounts to a 20% underestimate of evolution at  $z = 0.3$  and a 70% underestimate at  $z = 0.8$  for  $n = -1.5$ .

These uncertainties are relatively minor compared to the expected amount of evolution. For example, if  $n = -1.5$  and  $\nu_c(T, z = 0) \approx 3.2$ , we expect  $C(T, z = 0.3) \approx 0.3$  and  $C(T, z = 0.8) \approx 0.03$ . Larger values of  $\nu_c$ , characteristic of hotter clusters, lead to even more evolution. Because these evolution predictions are over an order of magnitude larger than the systematic errors,  $M_{\text{vir}}-T_X$  normalization discrepancies do not seriously affect the conclusion that cluster temperature evolution rules out  $\Omega_M = 1$ , particularly when clusters at  $z > 0.5$  are included.

Partially because of the potentially significant uncertainty in  $\sigma_8$ , certain authors have been cautious about the conclusions that can be drawn about  $\Omega_M$  from cluster temperature evolution (Colafrancesco, Mazzotta, & Vittorio 1997; Viana & Liddle 1999; Borgani et al. 1999b). However, maximum likelihood methods of determining  $\Omega_M$  that compare the cluster temperature function at  $z \approx 0$  directly with the cluster temperature function at higher redshifts (e.g., Henry 1997; Donahue & Voit 1999) can obtain stronger constraints on  $\Omega_M$  because they are differential measurements in which much of the uncertainty in  $\sigma_8$  and  $\delta_c$  cancels. Figure 4 shows the cluster evolution predictions that result when a representative range of  $\sigma_8$  values is considered. Here we allow  $0.5 \leq \sigma_8 \Omega_M^{0.47-0.1\Omega_M} \leq 0.6$ . At the  $z \approx 0.3$  redshift of the Henry (1997) clusters the prediction of the high- $\sigma_8$ ,  $\Omega_M = 1$  model is only a factor of two lower than the low- $\sigma_8$ ,  $\Omega_M = 0.5$  model, underscoring the need to identify systematic sources of uncertainty in  $\sigma_8$  before deriving evolutionary predictions for clusters from it. However, Figure 5 paints a somewhat rosier picture. Here we allow  $\nu_{c0} = \nu_c(5 \text{ keV}, z = 0)$  to span a range that corresponds to a factor of two range in the mass normalization at 5 keV, or equivalently, a factor of two range in the number density of 5 keV clusters at  $z = 0$ . The resulting systematic uncertainty in the best-fitting  $\Omega_M$  is  $\lesssim 0.1$ .

#### 4.4. Toward Greater Precision

When using Press-Schechter methods to model cluster evolution, one should always keep in mind that they are useful because they efficiently approximate numerical simulations. Our confidence in these methods is rooted in the fact that they reproduce the mass function of simulated clusters reasonably well. Less work has been done on comparisons of simulated cluster temperature functions with temperature functions derived from Press-Schechter mass functions using an  $M_{\text{vir}}-T_X$  relation (e.g., Bryan & Norman 1998, Pen 1998).

Given the ambiguities surrounding the  $M_{\text{vir}}-T_X$  relation and the very definition of a cluster’s mass, the most robust way to model the evolution of  $dn/dT$  would seem to be with a version of the Press-Schechter formalism that describes the temperature function directly. In such a scheme, one would separate the function  $\nu_c(T, t)$  that determines the evolution of  $dn/dT$  into a temperature-dependent part  $\nu_c(T, 0)$  and a time-dependent part  $g(t; \Omega_M, \Omega_\Lambda)$ . In principle,  $g(t; \Omega_M, \Omega_\Lambda)$  could be derived from a grid of simulated cluster temperature functions. However, creating such a simulation set would be very expensive. The simulation volume would need to be extremely large to obtain adequate statistics on rare, high-temperature clusters.

Maximum likelihood fits to cluster temperature surveys are essentially seeking the best-fitting  $\nu_c(T, z) = \nu_c(T, 0)g(z; \Omega_M, \Omega_\Lambda)$ . Figure 5 shows that this technique is fairly robust with respect to systematic uncertainties in the  $M_{\text{vir}}-T_X$  normalization. Statistical uncertainties in the normalization and slope of  $\nu_c(T, 0)$  are handled naturally by the maximum likelihood method. Insofar as the dependence of  $\nu_c(T, z)$  on cosmological parameters is accurate, this technique currently has the potential to deliver values of  $\Omega_M$  that are accurate to  $\lesssim 0.1$ . However, it remains to be seen how accurately our assumed forms for  $g(z; \Omega_M, \Omega_\Lambda)$  reproduce the results of large-scale clustering simulations.

### 5. Summary

X-ray surveys of distant clusters are placing increasingly more stringent constraints on  $\Omega_M$ . The lack of extreme evolution in the cluster temperature function strongly indicates that  $\Omega_M < 1$ . One of the crucial ingredients in placing such constraints on  $\Omega_M$  is the  $M_{\text{vir}}-T_X$  relation that converts cluster temperatures to cluster masses, enabling us to relate X-ray temperature surveys to theoretical models for cluster formation. If we are to extract accurate values of  $\Omega_M$  from the larger cluster temperature surveys expected from *Chandra* and *ASCA*, we need to ensure that our  $M_{\text{vir}}-T_X$  relation faithfully describes cluster evolution when coupled with Press-Schechter analysis. To that end, this paper has

analyzed our current understanding of the cluster mass-temperature relation in an effort to identify the systematic errors it introduces into measurements of cosmological parameters.

We find that the usual derivation of the  $M_{\text{vir}}-T_X$  relation, which assumes that clusters form by spherical top-hat collapse and that we are observing them immediately after they formed, is physically inconsistent. The rough agreement between the  $M_{\text{vir}}-T_X$  normalization derived in this way and the normalization determined from numerical models of clusters is therefore somewhat coincidental. To obtain the proper normalization, one needs to account both for the fact that much of a cluster’s mass accreted well before the moment we are observing it and for the non-zero density at  $r_{200}$ , which requires a surface pressure term to be included in the virial theorem.

Because of these shortcomings of the spherical top-hat picture, we advocate a more realistic scenario for deriving the  $M_{\text{vir}}-T_X$  relation in which clusters form quasi-continuously. An expression for the  $M_{\text{vir}}-T_X$  relation can be derived in the context of hierarchical merging, but the normalization of this relation depends on the concentration parameter  $c$  of the cluster, which must be obtained from simulations. The primary advantage of this form for the  $M_{\text{vir}}-T_X$  relation is that, unlike the spherical top-hat model, it properly reproduces the cessation of cluster evolution at late times if  $\Omega_M < 1$ .

Given the systematic uncertainties in setting the normalization of the  $M_{\text{vir}}-T_X$  relation, we have investigated their impact on the derivation of cosmological parameters from the cluster temperature function. Because two applications of the  $M_{\text{vir}}-T_X$  relation are needed to extract  $\sigma_8$ , this parameter is particularly susceptible to uncertainties in the mass-temperature normalization: a mass-normalization uncertainty of 50% leads to a 15% uncertainty in  $\sigma_8$ . However, only a single application of the  $M_{\text{vir}}-T_X$  relation is needed to extract  $\Omega_M$ , making it less vulnerable to normalization uncertainties. The systematic error in  $\Omega_M$  owing to uncertainties in the  $M_{\text{vir}}-T_X$  relation is  $\sim 0.1$ .

Improvements in our understanding of the  $M_{\text{vir}}-T_X$  relation await comparisons of theoretically-derived cluster temperature functions with structure-formation simulations large enough to contain many hot clusters. In essence, the  $dn/dT$  expression derived from the  $M_{\text{vir}}-T_X$  relation and the Press-Schechter mass function is no more than an elaborate fitting formula for representing the results of simulations. The ideal mass-temperature relation will therefore be the one that reproduces simulated temperature functions or velocity-dispersion functions most accurately. Even better would be a fitting formula that gives  $dn/dT$  directly without passing through murky intermediate steps involving ill-defined cluster masses. Until we have resolved these systematic uncertainties in deriving  $dn/dT$ , our constraints on  $\Omega_M$  from cluster temperatures will not grow appreciably tighter.

Megan Donahue’s support, encouragement, and advice has been invaluable to the author, who would also like to acknowledge Pat Henry, Stefano Borgani, and the referee for helpful comments and NASA grants NAG5-3257 and NAG5-3208 for partial support.

## APPENDIX CONTINUOUS CLUSTER GROWTH IN $\Omega_M < 1$ UNIVERSES

In the spirit of Gunn & Gott (1972), we can idealize continuous cluster growth as occurring through the sequential collapse and virialization of an infinite series of concentric shells, each obeying the equation of motion

$$\ddot{R} = -\frac{GM}{R^2} + \frac{\Lambda R}{3} , \quad (1)$$

where  $R$  is the radius of the shell encompassing mass  $M$ , and  $\Lambda$  is the cosmological constant. The specific energy of the matter in the shell is then

$$\epsilon = \frac{\dot{R}^2}{2} - \frac{GM}{R} - \frac{\Lambda R^2}{6} , \quad (2)$$

which remains constant until the shell virializes. If the shell ever reaches the critical radius  $R_{\text{cr}} = (3GM/\Lambda)^{1/3}$ , cosmic repulsion dominates gravity from then on, and the shell never collapses.

We can cast the equation of motion for the shell into dimensionless form by defining  $x = R/R_{\text{cr}}$ ,  $\theta = \Lambda^{1/2}t$ , and  $\xi = \epsilon R_{\text{cr}}^{-2} \Lambda^{-1}$ , so that

$$\frac{dx}{d\theta} = \left[ \frac{2}{3x} + 2\xi + \frac{x^2}{3} \right]^{1/2} . \quad (3)$$

A particular shell will collapse if  $x_0^3 + 6\xi x_0 + 2 = 0$  for some  $x_0$  in the range  $0 \leq x_0 < 1$ . Solving this cubic equation, we find

$$x_0 = 2^{3/2} |\xi|^{1/2} \cos \left( \frac{\alpha_\xi}{3} - \frac{2\pi}{3} \right) , \quad (4)$$

where  $\alpha_\xi$  is defined by  $\cos \alpha_\xi = -(8|\xi|^3)^{-1/2}$  with  $\pi/2 \leq \alpha_\xi \leq \pi$ . The shell therefore reaches its maximum radius  $R_{\text{cr}} x_0(\xi)$  at a time  $\Lambda^{-1/2} \theta_0(\xi)$ , where

$$\theta_0(\xi) = \int_0^{x_0(\xi)} \frac{x^{1/2} dx}{\left( \frac{x^3}{3} + 2\xi x + \frac{2}{3} \right)^{1/2}} . \quad (5)$$

Because of the symmetry of the motion, the shell collapses to the origin at  $t_c(\xi) = 2\Lambda^{-1/2}\theta_0(\xi)$ , which we will take to be the time of virialization.

The overall scale factor of the universe obeys a similar equation of motion, for which the specific energy of the background matter is

$$\epsilon_b = \frac{\dot{a}^2}{2} - \frac{H_0^2}{2}\Omega_M a^{-1} - \frac{H_0^2}{2}\Omega_\Lambda a^2 \quad (6)$$

$$= \frac{H_0^2}{2}(1 - \Omega_M - \Omega_\Lambda) . \quad (7)$$

The universe changes from decelerating to accelerating when  $a = a_{\text{cr}} \equiv (\Omega_M/2\Omega_\Lambda)^{1/3}$ , and with the definition  $w = a/a_{\text{cr}}$ , the dimensionless equation of motion for the background expansion becomes

$$\frac{dw}{d\theta} = \left[ \frac{2}{3w} + 2\xi_b + \frac{w^2}{3} \right]^{1/2} , \quad (8)$$

where  $\xi_b = \epsilon_b a_{\text{cr}}^{-2} \Lambda^{-1}$ .

Taking advantage of the formal similarities between these equations of motion, we can derive an expression for perturbation growth in an open universe. In the linear regime,  $\delta\rho/\rho = -3\delta w/w$ , where  $\delta w = x - w$ , and at any moment in time we have

$$\int_0^x \frac{y^{1/2} dy}{(y^3 + 6\xi y + 2)^{1/2}} = \int_0^w \frac{y^{1/2} dy}{(y^3 + 6\xi_b y + 2)^{1/2}} , \quad (9)$$

At early times, when  $x^3 + 2 \gg |6\xi x|$  and  $w^3 + 2 \gg |6\xi_b w|$ , we obtain

$$\frac{\delta\rho}{\rho} = 9(\xi_b - \xi) \frac{(w^3 + 2)^{1/2}}{w^{3/2}} \int_0^w \frac{y^{3/2} dy}{(y^3 + 2)^{3/2}} , \quad (10)$$

and at the earliest times ( $w \ll 1$ ), this expression reduces to

$$\frac{\delta\rho}{\rho} = \frac{9}{5}(\xi_b - \xi)w . \quad (11)$$

Perturbations at early times grow like  $1/(1+z)$ , as expected, and their amplitudes are proportional to the specific energy difference between the perturbation and the background. Note that if the universe is flat, the background specific energy  $\xi_b$  vanishes, and the perturbation amplitude within a shell is directly proportional to the shell's specific energy.

In the case of a vanishing cosmological constant, we can relate the perturbation amplitudes explicitly to their collapse times  $t_c$ . When the cosmological constant is very

small, we have  $|\xi| \gg 1$  and  $t_c \approx (\pi/3\sqrt{2})|\xi|^{-3/2}\Lambda^{-1/2}$ , so a shell that collapses and virializes at time  $t_c$  carries with it a specific energy

$$\epsilon = -\frac{1}{2} \left( \frac{2\pi GM}{t_c} \right)^{2/3} . \quad (12)$$

If we define  $t_\Omega = \pi\Omega_M/H_0(1 - \Omega_M - \Omega_\Lambda)^{3/2}$ , then at very early times,

$$\frac{\delta\rho}{\rho} \approx \frac{3}{2} \frac{(12\pi)^{2/3}}{10} \left( \frac{t}{t_\Omega} \right)^{2/3} \left[ 1 + (t_\Omega/t_c)^{2/3} \right] . \quad (13)$$

According to Lacey & Cole (1993), the growth rate for linear perturbations in this limit is  $D(t) \approx [(12\pi)^{2/3}/10](t/t_\Omega)^{2/3}$ , and we retrieve their expression for  $\delta_c(t)$ :

$$\delta_c(t) = \frac{3}{2} D(t) \left[ 1 + (t_\Omega/t)^{2/3} \right] . \quad (14)$$

Time therefore enters the Press-Schechter formula via the parameter  $\nu_c \propto \delta_c(t)/D(t) \propto [1 + (t_\Omega/t)^{2/3}]$ .

In the case of a flat universe with  $\Omega_M < 1$ , we have

$$\frac{\delta\rho}{\rho} = -9\xi D(t) \quad (15)$$

where

$$D(t) = D[w(t)] = \frac{(w^3 + 2)^{1/2}}{w^{3/2}} \int_0^w \frac{y^{3/2} dy}{(y^3 + 2)^{3/2}} , \quad (16)$$

in agreement with Eke et al. (1996). Inverting the function  $t_c(\xi)$  yields the function  $\xi_c(t)$  giving the specific energy  $\epsilon(t) = R_{cr}^2 \Lambda \xi_c(t)$  of a shell that collapses to the origin at time  $t$ . The collapse threshold becomes

$$\delta_c(t) = -9\xi_c(t) D(t) , \quad (17)$$

and time enters the Press-Schechter formula via  $\nu_c \propto \delta_c(t)/D(t) \propto \xi_c(t)$ .

## REFERENCES

- Bahcall, N. A., & Fan, X. 1998, ApJ, 504, 1  
 Bertschinger, E. 1985, ApJS, 58, 39  
 Binney, J., & Tremaine, S. 1987, Galactic Dynamics, Princeton: Princeton University Press  
 Blanchard, A., Sadat, R., Bartlett, J. G., & LeDour, M. 1999, astro-ph/990837

- Blanchard, A., & Bartlett, J. G. 1998, *A&A*, 332, 49L
- Borgani, S., Girardi, M., Carlberg, R. G., Yee, H. K. C., & Ellingson, E. 1999b, *ApJ*, 527, 561
- Borgani, S., Rosati, P., Tozzi, P., & Norman, C. 1999a, *ApJ*, 517, 40
- Bryan, G. L., & Norman, M. L. 1998, *ApJ*, 495, 80
- Carlberg, R. G., Yee, H. K. C., & Ellingson, E. 1997, *ApJ*, 478, 462
- Donahue, M. E., & Voit, G. M. 1999, *ApJ*, 523, 137L
- Donahue, M., Voit, G. M., Gioia, I., Luppino, G., Hughes, J. P., & Stocke, J. T. 1998, *ApJ*, 502, 550
- Donahue, M., Voit, G. M., Scharf, C. A., Gioia, I., Mullis, C. R., Hughes, J. P., & Stocke, J. T. 1999, *ApJ*, 527, 525
- Eke, V. R., Cole, S., & Frenk, C. S. 1996, *MNRAS*, 282, 263.
- Eke, V. R., Cole, S., Frenk, C. S., & Henry, J. P. 1998, *MNRAS*, 298, 1145
- Eke, V. R., Navarro, J. F., & Frenk, C. S. 1998, *ApJ*, 503, 569
- Evrard, A. E., Metzler, C. A. & Navarro, J. F. 1996, *ApJ*, 469, 494
- Fukuzawa, Y. 1997, Ph.D. thesis, Univ. Tokyo
- Girardi, M., Giuricin, G., Mardirossian, F., Mezzetti, M., & Boschin, W. 1998, *ApJ*, 505, 74
- Governato, F., Babul, A., Quinn, T., Tozzi, P., Baugh, C., Katz, N., & Lake, G. 1999, *MNRAS*, 307, 949
- Gunn, J. E., & Gott, J. R. 1972, *ApJ*, 176, 1
- Henry, J. P., & Arnaud, K. A. 1991, *ApJ*, 372, 410
- Henry, J. P. 1997, *ApJ*, 489, L1
- Hjorth, J., Oukbir, J., & van Kampen, E. 1998, *MNRAS*, 298, L1
- Horner, D. J., Mushotsky, R. F., & Scharf, C. A. 1999, *ApJ*, 520, 78
- Kitayama, T., & Suto, Y. 1996, *ApJ*, 469, 480
- Lacey, C., & Cole, S. 1994, *MNRAS*, 271, 676
- Lacey, C., & Cole, S. 1993, *MNRAS*, 262, 627
- Markevitch, M. 1998, *ApJ*, 504, 27
- Navarro, J. F., Frenk, C. S., & White, S. D. M. 1997, *ApJ*, 490, 493
- Oukbir, J., & Blanchard, A. 1992, *A&A*, 262, L21

- Oukbir, J., & Blanchard, A. 1997, *A&A*, 317, 1
- Peebles, P. J. E. 1993, *Principles of Physical Cosmology*, Princeton: Princeton University Press
- Pen, U. 1998, *ApJ*, 498, 60
- Press, W., & Schechter, P. 1974, *ApJ*, 187, 425
- Shapiro, P. R., Iliev, I. T., & Raga, A. C. 1999, *MNRAS*, 307, 203
- Viana, P. T. P., & Liddle, A. R. 1996, *MNRAS*, 281, 323
- Viana, P. T. P., & Liddle, A. R. 1999, *MNRAS*, 303, 535
- Voit, G. M., & Donahue, M. 1998, *ApJ*, 500, L111



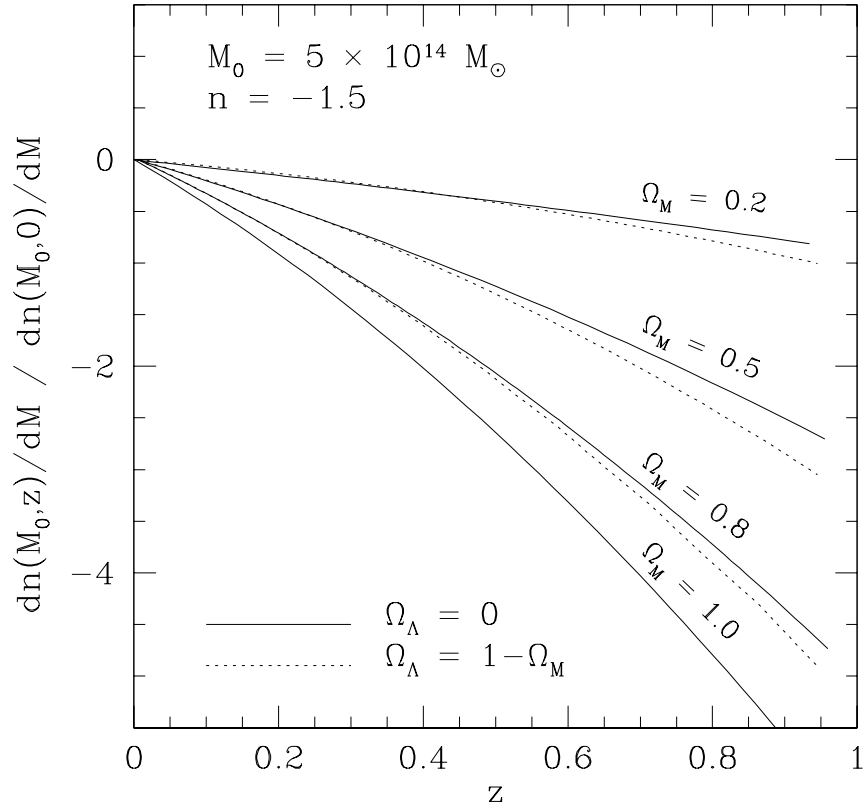


Fig. 1.— Expected evolution of massive clusters at mass scale  $M_0$  for different values of  $\Omega_M$ .

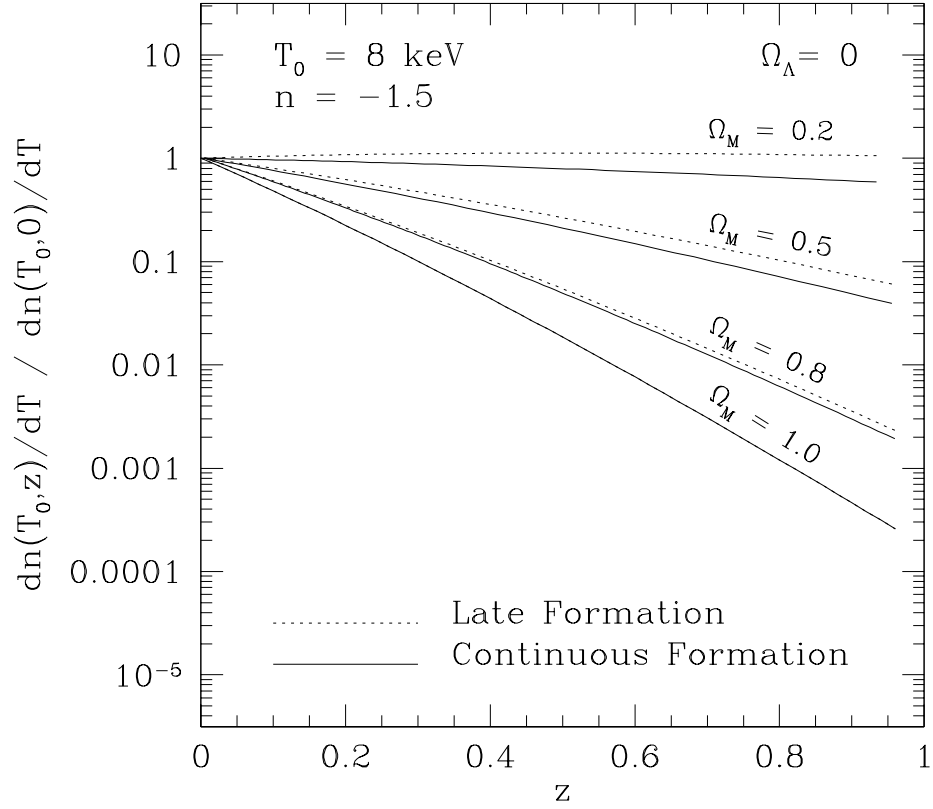


Fig. 2.— Expected evolution in the comoving number density of 8 keV clusters for the late-formation approximation and the continuous formation approximation. If  $\Omega_M \approx 0.2$ , the best-fitting  $\Omega_M$  for the late-formation and continuous-formation cases can differ by  $\sim 0.1$ .

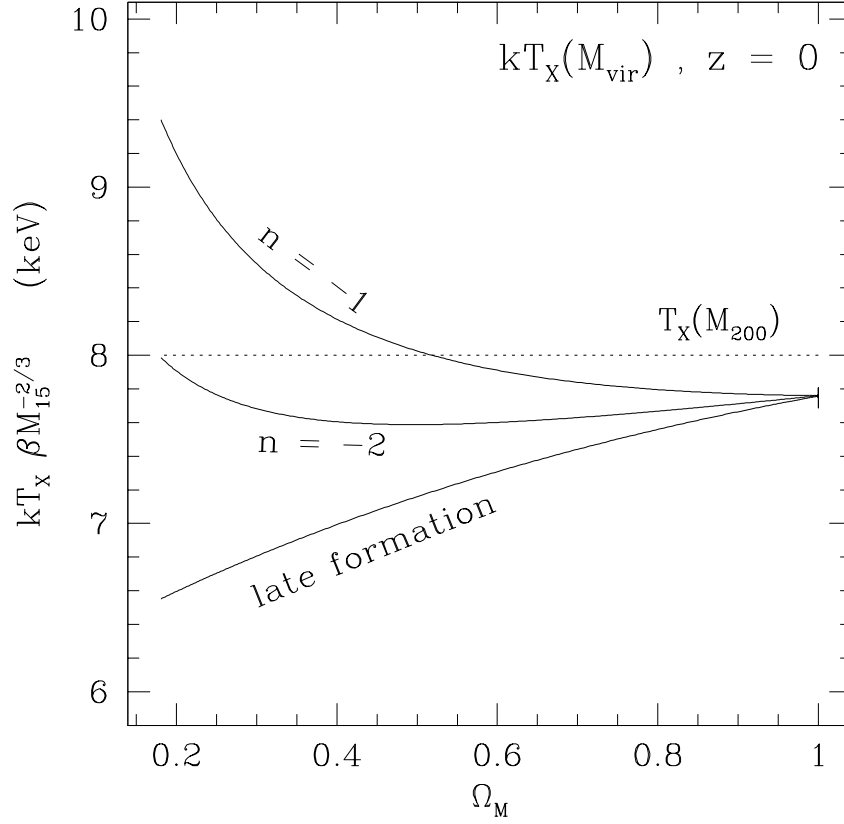


Fig. 3.— Dependence of the  $M_{\text{vir}}-T_X$  normalization on  $\Omega_M$ . The dotted line represents the temperature of a cluster containing  $10^{15} h^{-1} M_\odot$  cluster within the radius  $r_{200}$ , as predicted by the simulations of Evrard et al. (1996). The solid line labeled “late formation” shows the temperatures predicted by  $M_{\text{vir}}-T_X$  relation of Eke et al. (1996), and the other two solid lines represent the  $M_{\text{vir}}-T_X$  relations from Voit & Donahue (1998) for  $n = -1$  and  $-2$ .

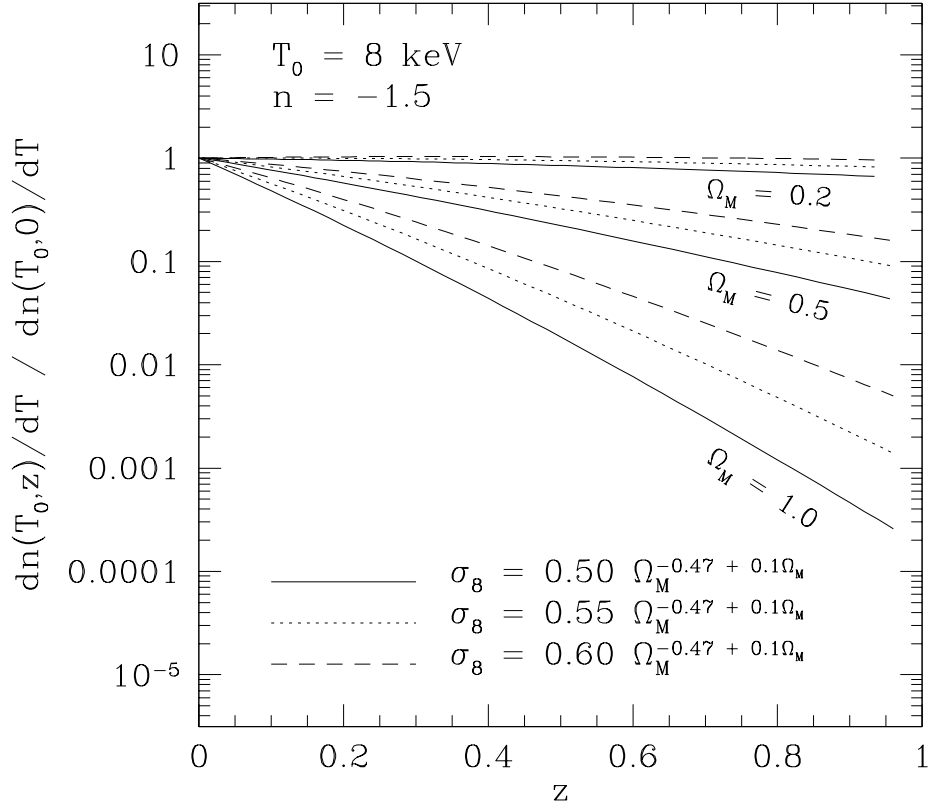


Fig. 4.— Expected evolution in the comoving number density of 8 keV clusters for  $0.5 \leq \sigma_8 \Omega_M^{0.47-0.1\Omega_M} \leq 0.6$ . Because of uncertainties in the  $M_{\text{vir}}-T_X$  relation,  $\sigma_8$  is not tightly constrained by the cluster temperature function. If these uncertainties are taken at face value, they result in a considerable spread in predictions for cluster evolution.

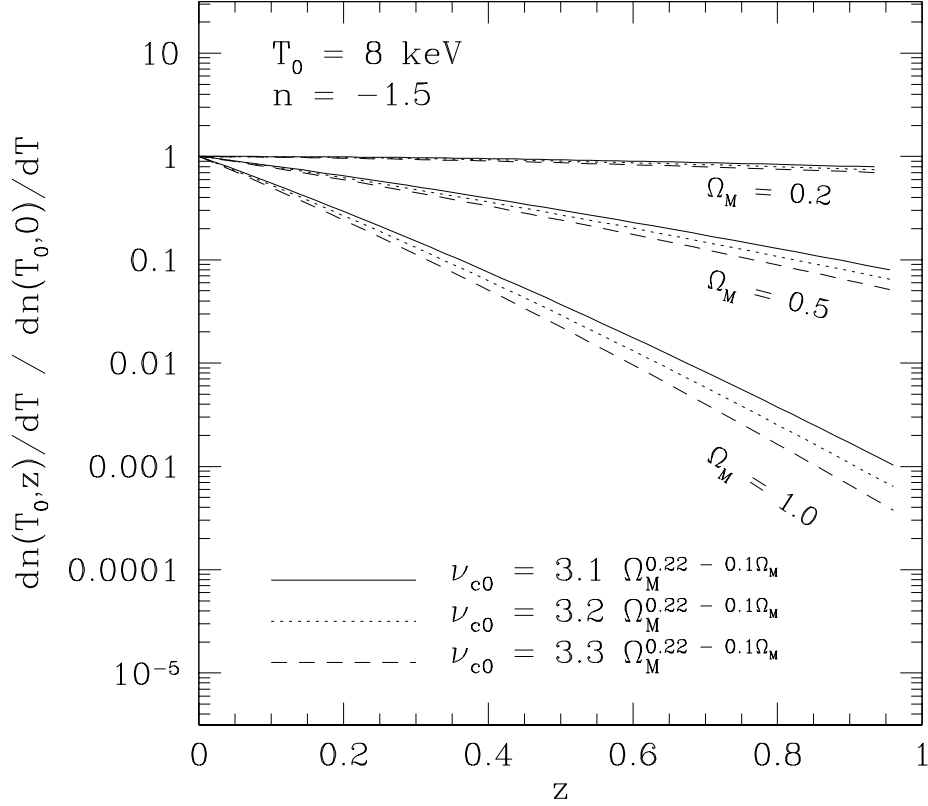


Fig. 5.— Expected evolution in the comoving number density of 8 keV clusters over the range of  $\nu_c$  values corresponding to the observed low-redshift cluster temperature function at 5 keV. Despite the uncertainties in the  $M_{\text{vir}}-T_X$  relation, the parameter  $\nu_{c0} = \nu_c(5 \text{ keV}, z = 0)$  is fairly well constrained. A 50% change in the mass-normalization, or correspondingly, a 50% change in the comoving number density of 5 keV clusters, changes the best fitting  $\nu_c$  by  $\sim 5\%$ . The resulting spread in predictions for cluster evolution is not as severe as one might have guessed from the uncertainties in  $\sigma_8$ .